5

Impacts of Surface Functionalization on the Electrocatalytic Activity of Noble Metals and Nanoparticles

Zhi-you Zhou and Shaowei Chen
Department of Chemistry and Biochemistry, University of California, Santa Cruz, CA, USA

1. Introduction

Low temperature fuel cells are a promising clean energy source, which can directly convert the chemical energy stored in hydrogen and small organic molecules (e.g., methanol, ethanol, and formic acid) into electrical energy with high efficiency, and thus find extensive applications in, for instance, automobiles and portable electronic devices. However, the commercialization of fuel cells is seriously impeded by the poor performance of the electrocatalysts for oxygen reduction reactions (ORR), and oxidation of small organic molecules.[1, 2] The sluggish kinetics of these reactions, even catalyzed by high loading of Pt-based catalysts, results in significant losses in thermal efficiency. Therefore, great efforts have been dedicated to improving the electrocatalytic performance of noble metals in the past decades.

Traditionally, the studies of fuel cell electrocatalysts focus on the design and manipulation of the composition (or alloy), particle size and shape (or crystal planes exposed), where rather significant progress has been achieved.[3-9] For example, bifunctional PtRu alloy catalysts significantly decrease the self-poisoning of carbon monoxide (CO) in methanol oxidation.[10-12] Pt-monolayer catalysts and Pt–M (M = Fe, Co, Ni, Pd, etc.) alloyed catalysts have considerably improved the catalytic activity for ORR.[13, 14] The shape-controlled synthesis of nanocrystals, which can provide uniform surface sites, has also produced electrocatalysts with good activity and selectivity.[15-17]

Recently, there emerges another promising strategy to tune electrocatalytic performances, i.e., modification of noble metal surfaces by deliberate chemical functionalization with specific molecules/ions. Organic ligands (such as poly(vinylpyrolidone) (PVP), cetyl trimethylammonium bromide (CTAB), and oleylamine) are often used in solution-phase syntheses of metal nanoparticles to control particle size, structure, and stability.[18] However, for applications in fuel cell catalysis, the ligands are either removed from the nanoparticle surface prior to use, or are simply considered as part of the supporting matrix.[19, 20] It is well-known that chemically modified electrodes can greatly improve the sensitivity and selectivity for electroanalytic reactions.[21-23] This suggests that the modification of specific molecules/ions on metal surfaces may also improve the electrocatalytic properties by virtue of the interactions between reactants and modifying molecules/ions.

Generally, there are several possible interactions between reactants (and spectator molecules/ions) and modifying molecules, as depicted in Figure 1: (1) Steric blocking effect. The modifying molecules occupy part of the metal surface, which can greatly hinder the adsorption of other molecules with a relatively large size that need multiple surface sites. (2) Electrostatic effects or dipole–dipole interactions. For example, the modification of anions (cations) may enhance the co-adsorption of cations (anions). (3) Electronic structure effects. The interactions between modifying molecules and metal atoms may result in adsorbate-induced distortions of the surface lattice and partial electron transfer, which may alter the adsorption energy of a second adsorbate.

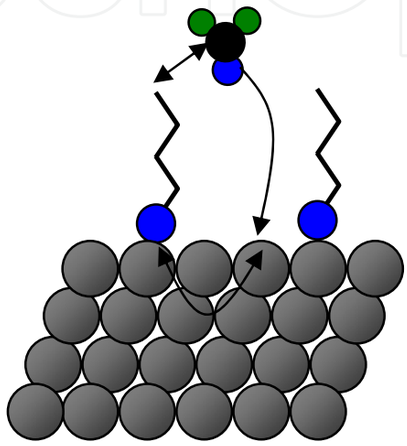

Fig. 1. Possible interactions between the reactants and modifying molecules on metal surfaces.

In this chapter, we highlight some recent key progress in surface functionalization on massive Pt single crystal planes with calixarene and CN^- ions, and their effects on the electrocatalytic activity and selectivity in ORR, hydrogen oxidation reactions (HOR), and methanol oxidation. We then extend the discussion to the synthesis of Pt and Pd nanoparticles capped with aryl and phosphine derivatives, and discuss the impacts of the molecule-molecule and molecule-nanoparticle interactions on the catalytic activities.

2. Surface modification of massive single crystal planes

Metal single crystal planes have well-defined surface atomic arrangements. Fundamentally, the use of single crystal planes as model electrocatalysts is anticipated to lead to a better understanding of the reaction mechanisms, surface processes, etc.[24, 25]

2.1 Modification of Pt single crystal planes with calix[4]arene

The ideal electrocatalysts for fuel cells should have both good activity and stability. It has been observed that during shutdown and startup that are inevitable for, for instance, automobile applications, the performance of cathodic Pt/C catalysts degrades quickly.[26] Under these conditions, the undesired ORR will occur on the anode side that is originally designed only for hydrogen oxidation. This reverse polarity phenomenon will push the cathode potential up to 1.5 V in some regions, and result in quick corrosion of Pt

nanoparticles and carbon support. Clearly, it is very important to design selective anode catalysts that can efficiently suppress ORR while fully preserving the ability for HOR.

The Markovic group shows that chemically modified platinum with a self assembled monolayer of calix[4]arene molecules may meet this challenging requirement.[27] The structure of a calix[4]arene thiol derivative that they used is illustrated in Figure 2a. The wide rim containing sulfur atoms can firmly adsorb onto the Pt(111) terrace, leaving some edge or step sites (i.e., natural defects) and narrow terraces between the calix[4]arene

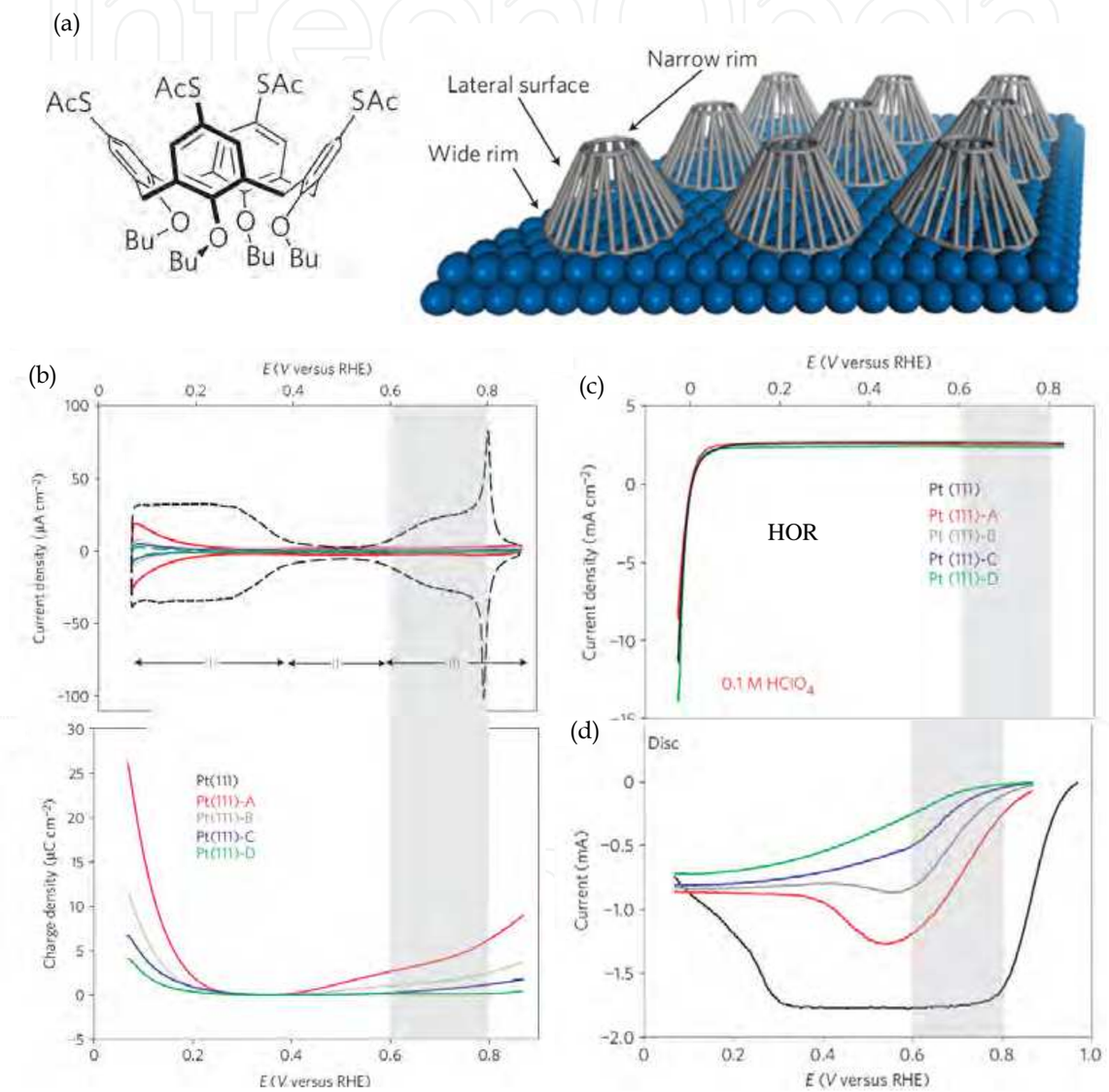

Fig. 2. (a) Structure and adsorption model for calix[4]arene molecules on Pt(111); (b) cyclic voltammograms of Pt(111) modified with different coverage (θ) of calix[4]arene molecules in 0.1 M $HClO_4$. θ increases from 0.84 to 0.98 (from curve A to D), calculated from the charge of hydrogen adsorption; HOR (c) and ORR (d) of calix[4]arene-modified Pt(111). Reprinted by permission from Macmillan Publishers Ltd: *Nature Materials* (2010, 9 (12), 998-1003), copyright 2010.

molecules. Cyclic voltammograms recorded in 0.1 M $HClO_4$ (panel b) indicate that the calix[4]arene molecules totally suppress the oxygen adsorption/desorption (+0.5 ~ +0.9 V), and most of hydrogen adsorption/desorption (+0.05 ~ +0.4 V), as their coverage increases from 0.84 to 0.98 (from curve A to D). This suggests that the ions/water from the supporting electrolyte are unable to penetrate the narrow rim of the calix[4]arene molecules, and the only sites available for the adsorption of electrolyte components are the relatively small number of unmodified Pt step-edges and/or the small ensembles of terrace sites between the anchoring groups.

The calix[4]arene-modified Pt(111) exhibits significantly different selectivity for ORR and HOR, as shown in panels (c) and (d). That is, ORR is greatly suppressed as the coverage of calix[4]arene increases, while HOR is essentially the same. It is accepted that the critical number of bare Pt atoms required for the adsorption of O_2 is higher than that required for the adsorption of H_2 molecules and a subsequent HOR. As for the ORR, the turnover frequency (TOF) of free Pt sites that are not occupied by calix[4]arene changes little (decreasing from 9 to 6 at +0.80 V), while the TOF for HOR increases sharply from 8 to 388 at +0.1 V as the coverage of calix[4]arene increases. Clearly, the decrease of ORR activity can be attributed to blocking effect, i.e., the calix[4]arene molecules block the adsorption of O_2 and its dissociation. However, the reason for enhanced HOR on the remaining Pt sites is not clear yet, and may be related to electronic effects, and/or mass-transfer limit for naked surfaces. The observed exceptional selectivity is not unique to the Pt(111)-calix system and has also been observed on Pt(100) and polycrystalline Pt electrodes, as well as Pt nanoparticles.[27, 28]

The successful preparation of oxygen-tolerant Pt catalysts for HOR indicates that surface functionalization of Pt surfaces is a promising approach to tuning the selectivity of electrocatalysts, which has great applications such as methanol-tolerant ORR catalysts.

2.2 Modification of Pt(111) with cyanide

Cyanide (CN^-) anions can adsorb strongly on metal surfaces. On the Pt(111) surface, they form a well defined ($2\sqrt{3} \times 2\sqrt{3}$)–R30° structure (inset to Figure 3a, denoted as Pt(111)–CN_{ad}).[29, 30] The structure consists of hexagonally packed arrays, each containing six CN groups adsorbed on top of a hexagon of Pt atoms surrounding a free Pt atom. The cyanide coverage is 0.5. The cyanide adlayer on Pt(111) is remarkably stable, and can survive even after repetitive potential cycling between +0.06 and +1.10 V (vs RHE).[31] The CN^- groups act as a third body, blocking Pt atoms that they occupy, but leaving other Pt atoms free onto which H, OH, or CO can still adsorb. The negative charge of the CN_{ad} dipole can also interact with other ions or polar molecules, so that the Pt(111)–CN_{ad} electrode has been considered as a chemically modified electrode.

Cuesta used the Pt(111)–CN_{ad} as a model catalyst to probe the reaction pathways of methanol electrooxidation.[32] As shown by the dashed curve in Figure 3a, there is no hysteresis of the oxidation current of methanol (+0.83 V) between the positive and the negative going sweeps on this surface. In addition, the hydrogen adsorption region (+0.05 ~ +0.5 V) remains unaffected in comparison with that recorded in a blank solution (solid curve). Electrochemical in situ FTIR studies confirm no CO formation in methanol oxidation on the Pt(111)–CN_{ad} electrode (Figure 3b). In addition to the product of CO_2 (~ 2340 cm^{-1})

and the original CN adlayer (~2100 cm^{-1}), no adsorbed CO signals can be observed in the region of 1800 to 2100 cm^{-1}.

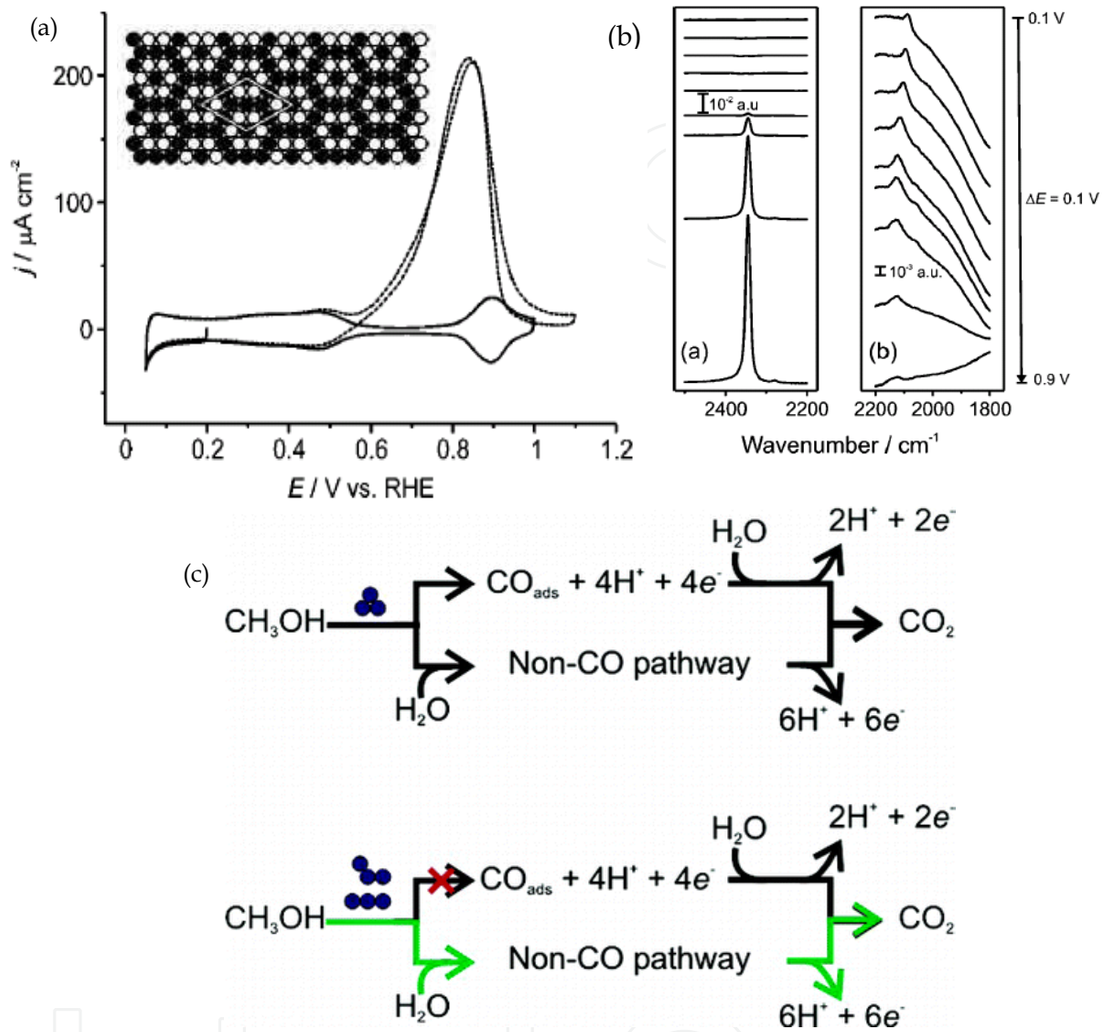

Fig. 3. (a) Cyclic voltammograms of Pt(111)–CN_{ad} electrode in 0.1 M $HClO_4$ (solid line) and 0.1 M $HClO_4$ + 0.2 M CH_3OH (dashed line). The inset is a model of the $(2\sqrt{3} \times 2\sqrt{3})$-R30° structure for a cyanide adlayer on Pt(111). Black circles correspond to Pt atoms, and white circles to linearly adsorbed CN^-. (b) Electrochemical in situ FTIR spectra of methanol oxidation on cyanide-modified Pt(111) electrode. No adsorbed CO can be detected. (c) Illustration of the reaction pathways of methanol oxidation on Pt. Reprinted with permission from *the Journal of the American Chemical Society* (2006, 128 (41), 13332-13333). Copyright 2006 American Chemical Society.

There are four possible free Pt sites on the Pt(111)–CN_{ad}: (i) a single Pt atom; (ii) two adjacent Pt atoms; (iii) three Pt atoms arranged linearly; (iv) three Pt atoms arranged forming a chevron with a 120° angle. No adsorbed CO formation on these reactive sites suggests that the dehydrogenation reaction of methanol to CO needs at least three contiguous Pt atoms, likely as triangle assembly (Figure 3c).

In another study, the Markovic group uses the Pt(111)–CN_{ad} as a model catalyst for ORR.[33] In acidic solutions, some anions such as SO_4^{2-} and PO_4^{3-} can adsorb strongly onto Pt surfaces (i.e., specific adsorption), and block surface sites for the adsorption of O_2. As a result, the ORR activity of Pt catalysts is much lower in H_2SO_4 (or H_3PO_4) than in $HClO_4$.[34] In the latter case, the adsorption of ClO_4^- is negligible. It has been found that if the Pt(111) electrode is modified with cyanide, the adsorption of SO_4^{2-} and PO_4^{3-} is greatly suppressed (Figure 4 a and b, Region II), and the butterfly peaks as well as the specific adsorption of SO_4^{2-} almost disappear. This can be simply understood in terms of through-space electrostatic repulsive interactions between the electronegative CN_{ad} adlayer and the negative SO_4^{2-} or PO_4^{3-}. However, the remaining free Pt sites on the Pt(111)–CN_{ad} are still accessible for hydrogen and oxygen adsorption, as indicated by the current between +0.05 and +0.5 V and the pair of voltammetric peaks at +0.90 V. More importantly, these free metal sites are sufficient for the chemisorption of O_2 molecules and to break the O–O bond, as demonstrated by the ORR activity of the Pt(111)–CN_{ad} electrode in 0.05 M H_2SO_4 (red solid curve, Figure 4c) similar to that of the naked Pt(111) in 0.1 M $HClO_4$ (grey dashed curve). It is determined that in comparison with naked Pt(111) (black solid curve), the ORR activity on Pt(111)–CN_{ad} shows a 25-fold increase in the H_2SO_4 solution, and a ten-fold increase in H_3PO_4 solution due to less suppression of PO_4^{3-} adsorption (Figure 4d).

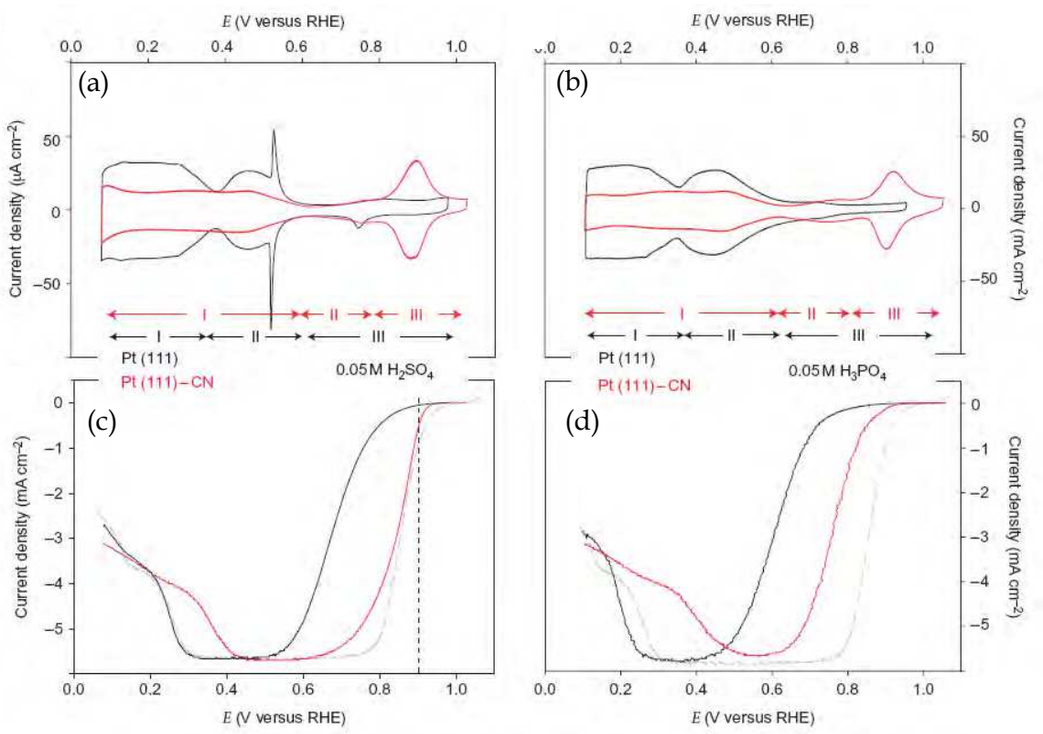

Fig. 4. Electrochemical measurements on CN-modified and unmodified Pt(111) surfaces in (a and c) 0.05 M H_2SO_4 and (b and d) 0.05 M H_3PO_4. (a and b) Cyclic voltammograms recorded in argon-saturated solutions. (c and d) ORR polarization curves in O_2 saturated solutions at 1600 rpm. Grey-dashed curves correspond to the ORR in 0.1 M perchloric acid. Reprinted by permission from Macmillan Publishers Ltd: *Nature Chemistry* (2010, 2 (10), 880-885), copyright 2010.

In a 0.1 M KOH solution, the behaviors change greatly. In this solution, the Pt(111)–CN_{ad} electrode shows a 50-fold decrease in ORR activity as compared to the naked electrode. The interaction between the CN_{ad} adlayer and the hydrated K^+ cations may lead to the formation of large $K^+(H_2O)_x$–CN_{ad} clusters, which are 'quasi-specifically adsorbed' on Pt, hence acting as large site blockers for the adsorption of reactants such as O_2 and H_2O (see Figure 5c).[35]

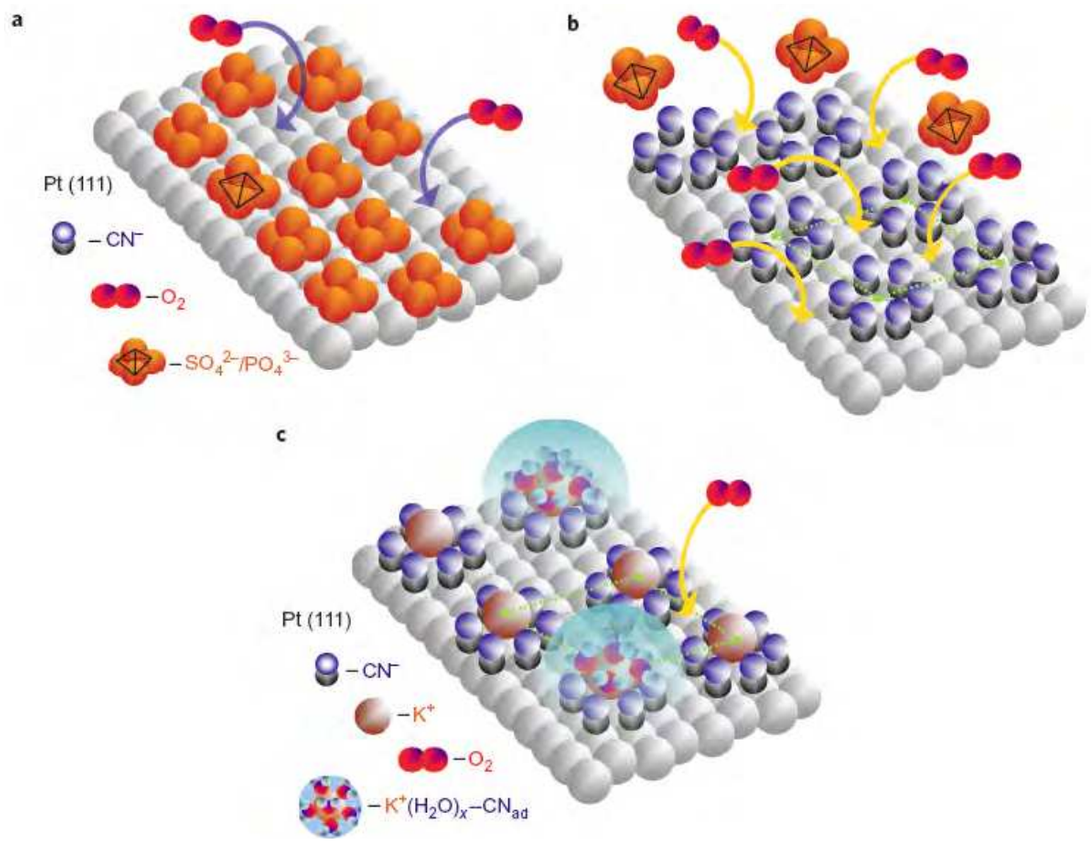

Fig. 5. Proposed models for the selective adsorption of spectator species and the available Pt surface sites for O_2 adsorption on CN-free and CN-covered Pt(111): (a) On Pt(111) covered by phosphoric/sulfuric acid anions O_2 can access the surfaces atoms only through a small number of holes in the adsorbate anion adlayer; (b) The number of holes required for O_2 adsorption is significantly increased on the Pt(111)–CN_{ad} surface because adsorption of phosphoric/sulfuric acid anions is suppressed by the CN adlayer so that the total CN_{ad}/OH_{ad} coverage is lower than the coverage by sulfuric or phosphoric acid anions; and (c) The adsorption of O_2 (and H_2O) is strongly suppressed on the Pt(111)–CN surface in alkaline solutions due to non-covalent interactions between K^+ and covalently bonded CN_{ad}, and the formation of spectator CN_{ad}–$M^+(H_2O)_x$ clusters. For clarity, the hydrated K^+ ions are shown as not being part of the double-layer structure. In reality, however, they are quasi-specifically adsorbed, with the locus centred between the covalently bonded CN_{ad} and hydrated K^+. Reprinted by permission from Macmillan Publishers Ltd: *Nature Chemistry* (2010, 2 (10), 880-885), copyright 2010.

The selective adsorption of spectator species and reactants and the impacts on ORR are summarized in Figure 5, where CN_{ad} repels the adsorption of SO_4^{2-} and PO_4^{3-} anions,

resulting in more surface sites for O_2 adsorption in acidic media (panels a and b), and interacts with hydrated K^+ cations to suppress the O_2 adsorption in KOH solution (panel c).

These studies of the interactions between the CN_{ad} adlayer and H_2O, oxygen species, and spectator anions shed light on the role of covalent and non-covalent interactions in controlling the ensemble of Pt active sites required for high turn-over rates of ORR and methanol oxidation, and may be helpful in the quest of identifying new directions in designing electrochemical interfaces that can bind selectively reactive and spectator molecules.

3. Surface-functionalization of metal nanoparticles with improved electrocatalytic properties

Surface functionalization of massive single crystal electrodes offers a unique structural framework for the fundamental studies of fuel cell electrocatalysis. Yet, from the practical points of view, the preparation of surface-functionalized metal nanoparticles is necessary. In fact, most catalysts are in the form of nanosized particles dispersed on varied substrate supports. Herein, we highlight two cases, i.e., aryl- and phosphine-stabilized Pt and Pd nanoparticles, and their applications in fuel cell electrocatalysis.

3.1 Surface functionalization by aryl groups

The modification of electrode surfaces with aryl groups through electrochemical reduction of diazonium salts has been studied rather extensively.[36] A variety of electrode substrates, such as carbon, silicon, copper, iron, and gold, have been used. The covalent attachment of the aryl fragments onto the electrode surfaces is via the following mechanism[37]

$$Ar\text{-}N{\equiv}N^+ + e \rightarrow Ar^\bullet + N_2 \quad (1)$$

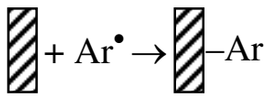

(2)

At a negative enough potential, diazonium ions are electrochemically reduced to aryl radicals releasing nitrogen molecules (step (1)). The radicals are very active, and they are readily bonded onto the electrode surfaces (step (2)). Theoretical calculations predict that the adsorption energies vary from 25 to 106 kcal mol^{-1} on different substrates.[37] The strong bond strength suggests that the interaction is chemical in nature, i.e., covalent bond.

In recent years, aryl-stabilized metal nanoparticles through metal-carbon (M-C) covalent bonds, synthesized by the co-reduction of metal precursors and diazonium salts, have received great interest.[37-39] The formation mechanism is similar to that in electrochemical reduction.[36, 38] For instance, for Au nanoparticles, surface enhanced Raman scattering (SERS) have provided direct evidence for the formation of Au-C covalent bonds on the nanoparticle surface.[40]

Mirkhalaf and co-workers are the first to report the synthesis of Au and Pt nanoparticles stabilized by 4-decylphenyl fragments through the co-reduction of the corresponding metal precursors and diazonium salt.[38] The resulting Pt nanoparticles show a smaller core

diameter (~ 3 nm) than the Au nanoparticles (8.1 nm), due to the stronger bonding of the aryl group on Pt than on Au. The ^{1}H NMR spectra of the Pt nanoparticles in CD_2Cl_2 solution only show some very board peaks from the 4-decylphenyl ligands. The broadening of the NMR peaks is ascribed to the fast spin-spin relaxation of atoms close to the metal core, and confirms the direct linkage of the 4-decylphenyl fragments onto Pt surfaces.

Using a similar method, our group has synthesized Pd nanoparticles stabilized by a variety of aryl moieties, including biphenyl, ethylphenyl, butylphenyl, and decylphenyl groups.[39, 41] Of these, the average core size of the Pd nanoparticles stabilized by butylphenyl group (Pd-BP) is 2.24 ± 0.35 nm (Figure 6a and b),[41] which is much smaller than that of commercial Pd black catalyst (10.4 ± 2.4 nm, Figure 6c and d). Thermogravimetric analysis (TGA) indicates that the organic component is about 19% with a main mass-loss peak at 350 °C (Figure 7a). On the basis of the weight loss and the average core size of the Pd nanoparticles, the average area occupied by one butylphenyl ligand on the Pd nanoparticle surface is estimated to be about 21 Å^2, close to the typical value (~20 Å^2) for long-chain alkanethiolate adsorbed on metal nanoparticles.[42]

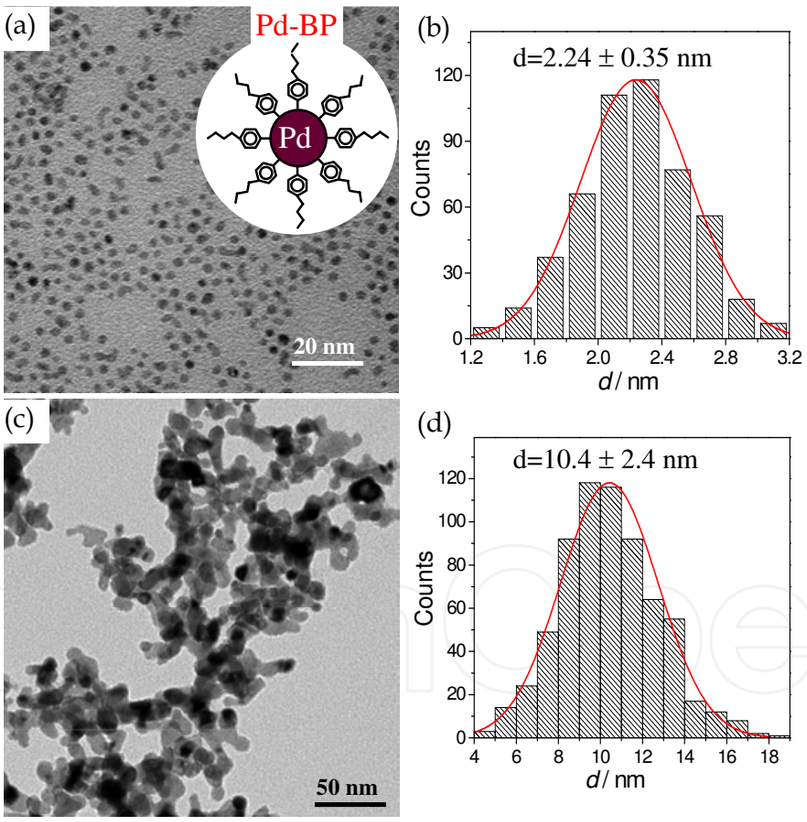

Fig. 6. TEM images and core size histograms of (a and b) Pd-BP nanoparticles and (c and d) commercial Pd black. Reprinted by permission from *Chemical Communications* (2011, 47 (21), 6075-6077). Copyright 2011 Royal Society of Chemistry.

The infrared spectrum of the Pd-BP nanoparticles (Figure 7b, curve A) shows the C-H vibrational stretch of the phenyl ring at 3027 cm^{-1}, and four aromatic ring skeleton vibrations at 1614, 1584, 1497, and 1463 cm^{-1}.[43] It is worth noting that the relative intensities of the

aromatic ring skeleton vibrations of the butylphenyl groups bound onto the Pd nanoparticles are significantly different from those of monomeric n-butylbenzene and 4-butylaniline (curves B and C). For instance, the strong band observed with n-butylbenzene at 1609 cm^{-1} and with 4-butylaniline at 1629 cm^{-1} becomes a very weak shoulder with Pd-BP, whereas the 1584 cm^{-1} band intensifies markedly with the ligands bound onto the nanoparticle surface. These observations suggest that the ligands on the Pd-BP surface are indeed the butylphenyl fragments by virtue of the Pd-C interfacial covalent linkage, and there are relatively strong electronic interactions between the aromatic rings and the Pd nanoparticles.

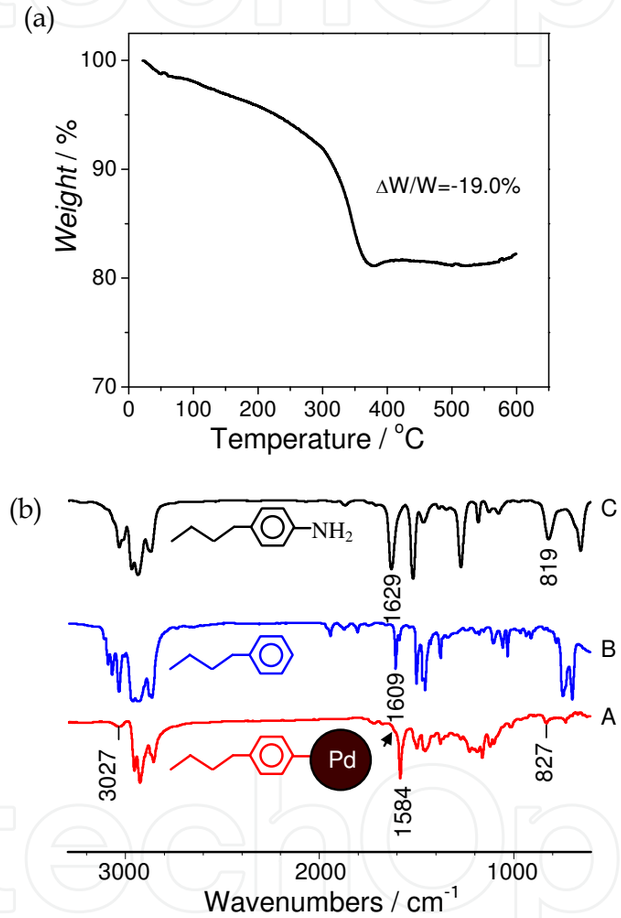

Fig. 7. (a) TGA curve of Pd-BP nanoparticles measured under a N_2 atmosphere at a heating rate of 10 ^oC min^{-1}. (b) FTIR spectra of (A) Pd-BP nanoparticles, (B) n-butylbenzene, and (C) 4-butylaniline. Reprinted by permission from *Chemical Communications* (2011, 47 (21), 6075-6077). Copyright 2011 Royal Society of Chemistry.

Cyclic voltammograms (Figure 8a) of Pd-BP nanoparticles recorded in 0.1 M H_2SO_4 indicates that the surface of the Pd-BP nanoparticles is fairly accessible for electrochemical reactions, since well-defined current peaks for the adsorption/desorption of hydrogen (–0.25 ~ 0.0 V) and oxygen (~ +0.30 V) can be observed. The specific electrochemical surface area (ECSA) of Pd, determined through the reduction charge of monolayer Pd surface oxide,

is estimated to be 122 m^2 g^{-1} for Pd-BP nanoparticles, which is about 3.6 times higher than that of commercial Pd black (33.6 m^2 g^{-1}). The theoretical ECSA of Pd-BP nanoparticles is calculated to be 223 m^2 g^{-1}, on the basis of the average core size (2.24 nm, Figure 6). This indicates that over 50% of the particle surface was accessible under electrochemical conditions.

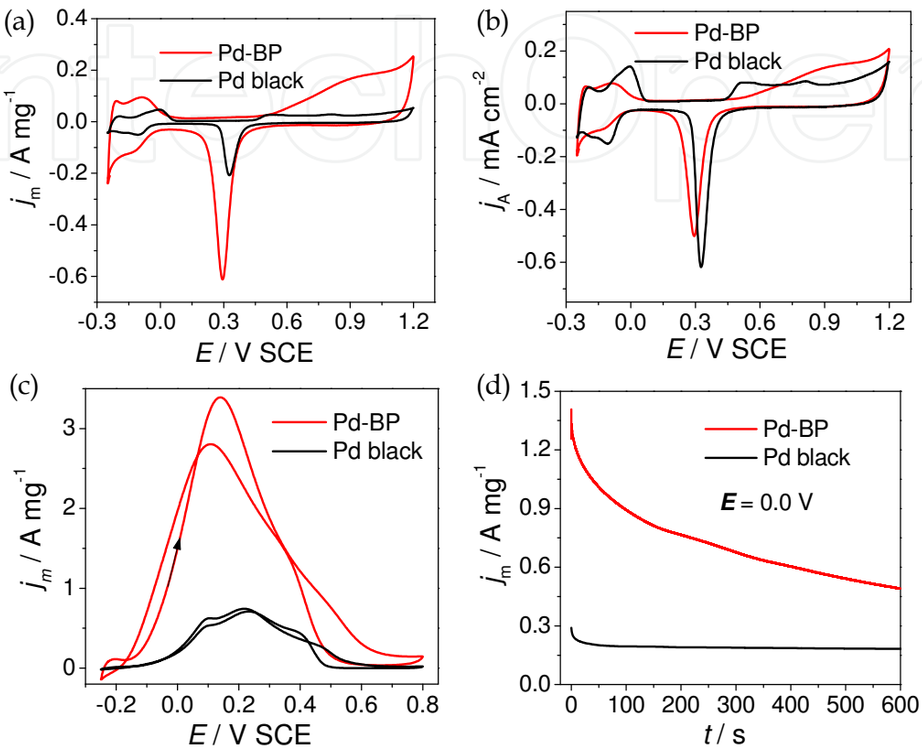

Fig. 8. Cyclic voltammograms of Pd-BP nanoparticles and commercial Pd black in 0.1 M H_2SO_4 with the currents normalized (a) by the mass loading of Pd and (b) by the effective electrochemical surface area at a potential scan rate of 100 mV s^{-1}. Panels (c) and (d) depict the cyclic voltammograms and current-time curves acquired at 0.0 V for HCOOH oxidation, respectively, at the Pd-BP nanoparticles and Pd black-modified electrode in 0.1 M HCOOH + 0.1 M H_2SO_4 at room temperature. Reprinted by permission from *Chemical Communications* (2011, 47 (21), 6075-6077). Copyright 2011 Royal Society of Chemistry.

Due to the remarkably high ECSA and surface functionalization, the Pd-BP nanoparticles exhibit a high mass activity in the electrocatalytic oxidation of formic acid. Figure 8c depicts the voltammograms of Pd-BP and Pd black catalysts recorded in a 0.1 M HCOOH + 0.1 M $HClO_4$ solution at a potential scan rate of 100 mV s^{-1}. The peak current density, normalized to the Pd mass, is as high as 3.39 A mg^{-1}_{Pd} on the Pd-BP nanoparticles, which is about 4.5 times higher than that of the Pd black (0.75 A mg^{-1}). In addition, the peak potential for HCOOH oxidation is also negatively shifted by 80 mV. The Pd-BP nanoparticles also possess higher stability of the voltammetric current than Pd black for formic acid oxidation. Figure 8d shows the current-time curves recorded at 0.0 V for 600 s. The Pd-BP catalysts maintain a mass current density that is 2.7 to 4.8 times higher than that of Pd black. The high electrocatalytic activity of Pd-BP nanoparticles may be correlated with butylphenyl

functionalization of the nanoparticle surface. As indicated by cyclic voltammograms where the currents are normalized to ECSA (Figure 8b), the adsorption of (bi)sulphate ions at around 0 V diminishes substantially on the Pd-BP electrode,[44] and the initial oxygen adsorption at around +0.50 V in the positive-going scan is also blocked, in comparison to Pd black. Such a discrepancy of surface accessibility and reactivity indicates that butylphenyl group may provide steric hindrance for (bi)sulphate adsorption, and also change the electronic structure of Pd.

Butylphenyl modified Pt (Pt-BP) nanoparticles have also been prepared by the co-reduction of diazonium salt and H_2PtCl_4 with $NaBH_4$ as the reducing agent.[45] TEM images (Figure 9) show that the as-prepared Pt-BP nanoparticles are well-dispersed and uniform, and well clear (111) lattice fringes can be observed. The average core size of Pt-BP nanoparticles is determined to be 2.93 ± 0.49 nm, which is comparable to the commercial Pt/C (3.1 nm) catalyst that is used in the controll experiment.

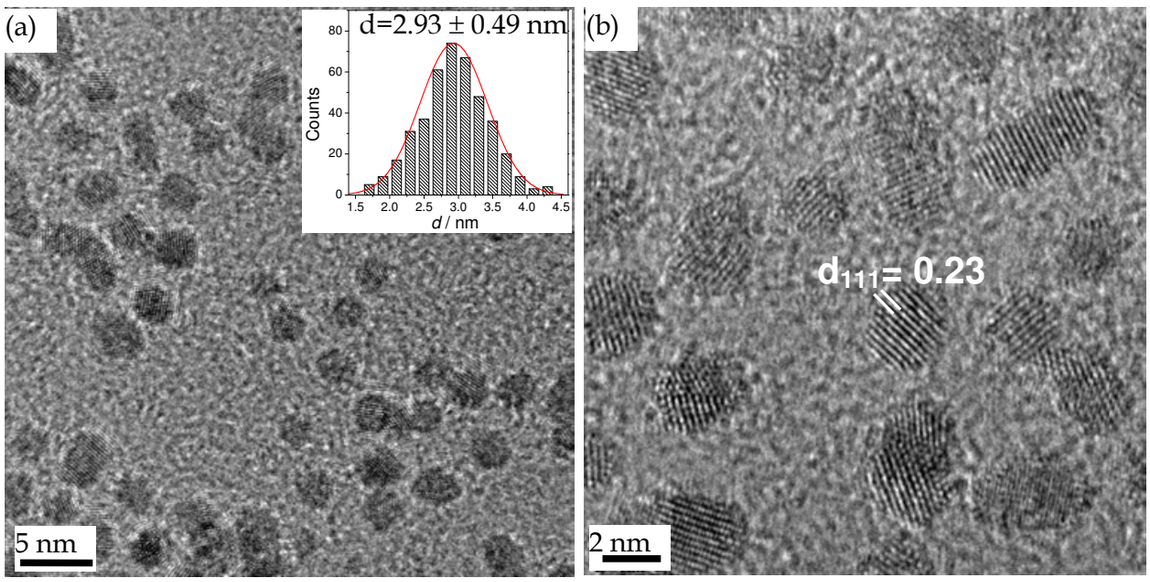

Fig. 9. TEM images of Pt-BP nanoparticles. Scale bars are 5 nm and 2 nm in panels (a) and (b), respectively. Inset to panel (a) shows the core size histogram. Reprinted by permission from *Physical Chemistry Chemical Physics* (2012, 14 (4), 1412-1417. Copyright 2012 Royal Society of Chemistry.

The IR transmission spectrum of Pt-BP nanoparticles also exhibits the characteristic peaks of the butylphenyl group, e.g., stretching vibration of the C–H moiety on the phenyl ring (3029 cm^{-1}), saturated C–H stretches in the butyl group (2955, 2929, 2858 cm^{-1}), aromatic ring skeleton vibration (1577 cm^{-1}), and out-of-plane C-H deformation vibration for para-substituted aromatic rings (827 cm^{-1}). The amount of ligands on the Pt-BP nanoparticles is quantitatively determined by TGA measurements to be about 27%. Therefore, the average area occupied by one butylphenyl ligand can be estimated to be about 5.8 $Å^2$, considerably lower than that observed with the aforementioned Pd nanoparticles.[41] Such a low occupied area of aryl group on Pt surfaces suggests there may exist some multilayer polyaryl structure.[46, 47]

It is well established that Pt catalysts for formic acid electrooxidation are easily poisoned by adsobed CO (CO_{ad}) intermediates.[25] Interestingly, the functionalization of Pt nanoparticles by the butylphenyl groups greatly suppresses the CO poisoning. Figure 10 compares the cyclic voltammograms of formic acid oxidation on the Pt-BP (red curve) and commercial Pt/C catalysts (black curve). On the Pt/C, along with increasing electrode potential, a weak and broad oxidation peak appears at around +0.30 V, followed by a sharp peak at +0.60 V in the forward scan. The former is attributed to the direct oxidation of formic acid to CO_2, while the latter is assigned to the oxidation of the CO_{ad} that is generated from the spontaneous dissociative adsorption of formic acid on Pt surfaces.[48] After the stripping of CO_{ad}, formic acid can then be readily oxidized on the clean Pt surface, as indicated by a very intensive current peak in the reverse scan. In contrast, on the Pt-BP nanoparticles, the hysteresis of the oxidation current of formic acid between forward and reverse scans is much less significant, and only a hump can be observed in the potential region around +0.60 V for CO_{ad} oxidation. This fact indicates that the CO poisoning pathway has been greatly suppressed on the Pt-BP nanoparticles. As a result, the peak current density of formic acid oxidation on the Pt-BP (1.03 A mg^{-1}_{Pt}) is about 4 times larger than that on the Pt/C (0.25 A mg^{-1}_{Pt}) in the forward scan at round +0.30 V.

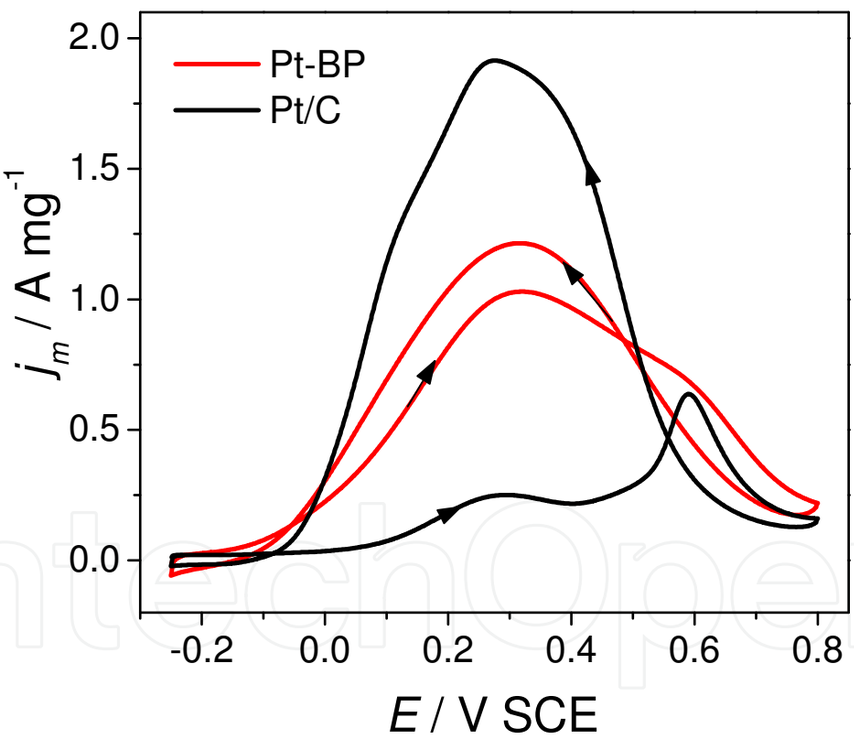

Fig. 10. Cyclic voltammograms of Pt-BP nanoparticles and commercial Pt/C catalyst in 0.1 M HCOOH + 0.1 M H_2SO_4 at 50 mV s^{-1}. Reprinted by permission from *Physical Chemistry Chemical Physics* (2012, 14 (4), 1412-1417). Copyright 2012 Royal Society of Chemistry.

The suppression of CO poisoning for formic acid on the Pt-BP nanoparticles is further confirmed by electrochemical in situ FTIR spectroscopic measurements (Figure 11). With Pt/C (panel b), the spectra show a downward band at 2343 cm^{-1} that is assigned to CO_2, the oxidation product of formic acid, and another at around 2050 cm^{-1} to linearly bonded CO

(CO_L), the poisoning intermediates. Clearly, unlike naked Pt, there is negligible adsorbed CO on the Pt-BP electrode (panel a), confirming that the functionalization of butylphenyl group have effectively blocked the poisoning pathway of formic acid oxidation. As a result, Pt-BP can yield more CO_2 than the Pt/C at a same potential.

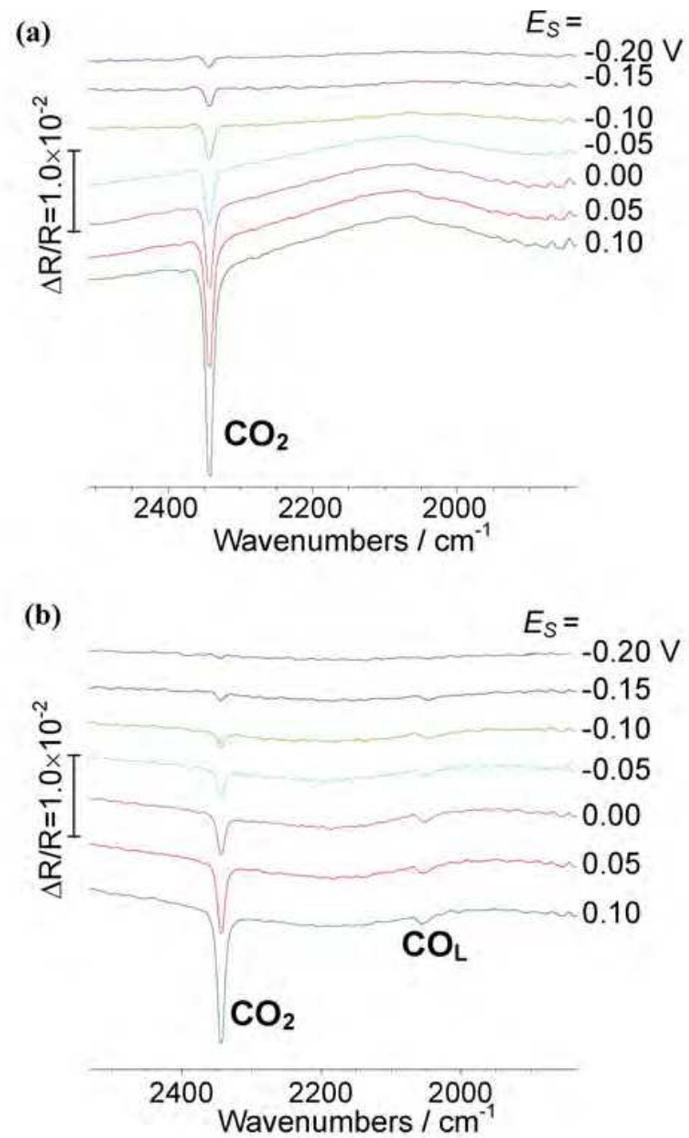

Fig. 11. Electrochemical in situ FTIR spectra of formic acid oxidation on the (a) Pt-BP nanoparticles and (b) commercial Pt/C catalyst in 0.1 M HCOOH + 0.1 M H_2SO_4 at different potentials. The sample potential (E_S) is varied from –0.20 to +0.10 V and the reference spectrum is acquired at E_R = –0.25 V. Reprinted by permission from *Physical Chemistry Chemical Physics* (2012, 14 (4), 1412-1417). Copyright 2012 Royal Society of Chemistry.

It has been known that there are at least two effects responsible for the improved electrocatalysts for formic acid oxidation: third-body effects and electronic structure effects.[49, 50] It is generally accepted that the dehydration of formic acid to form CO_{ad} is a site

demanding reaction, and several neighboring Pt sites are required.[50] Thus, this pathway can be blocked if Pt surfaces are covered by foreign atoms (third body). Clearly, the high catalytic activity of the Pt-BP nanoparticles may be, at least in part, reasonably attributed to third-body effects, i.e., the butylphenyl group provides steric hindrance for formic acid to form CO_{ad}.

The two examples listed above demonstrate that surface functionalization of noble metal nanoparticles with aryl groups is a promising route towards the preparation of electrocatalysts with improved performance for fuel cell electrocatalysis.

3.2 Surface functionalization by phosphine

Organophosphine ligands can strongly bind onto metal surfaces, especially for Pt group metals.[51, 52] Pietron and co-workers carry out electrochemical studies to examine the impacts of triphenylphosphine triphosphonate (TPPTP, Figure 12a) on the electrocatalytic activity of Pt nanoparticles for ORR.[53] The TPPTP-capped Pt nanoparticles are prepared through ligand exchange reactions between glycol-stabilized Pt nanoparticles and TPPTP for 2 to 4

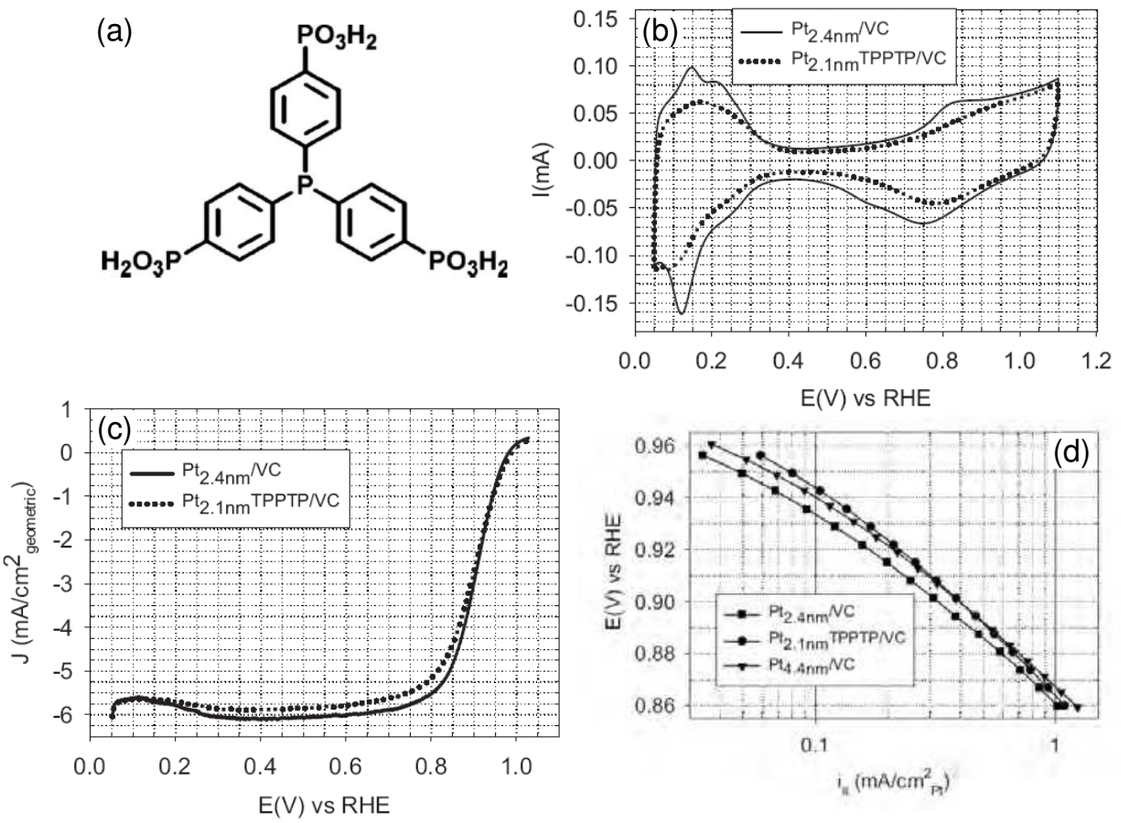

Fig. 12. (a) Molecular structure of TPPTP; (b) cyclic voltammograms of $Pt_{2.4\ nm}$/VC and $Pt_{2.2\ nm}$-TPPTP/VC in Ar-saturated 0.1 M $HClO_4$ at 25°C; (c) RDE voltammograms of the ORR; and (d) Tafel plots of the specific ORR activities at $Pt_{2.1\ nm}$-TPPTP/VC, and commercial $Pt_{2.4\ nm}$/VC and $Pt_{4.4\ nm}$/VC. Reprinted by permission from *Electrochemical and Solid State Letters* (2008, 11 (8), B161-B165). Copyright 2008 The Electrochemical Society.

days.[54] The core size of the Pt nanoparticles is about 2.1 nm. Studies based on X-ray absorption spectroscopy including XANES and EXAFS indicate that the coverage of TPPTP is about 0.3 ML, and the binding to Pt surfaces is via the P atom (Pt-P-P<tp) at +0.54 V (RHE), and approximately one-half of this converts to a Pt-O-P<tp linkage at +1.0 V.[55]

Electrochemical cyclic voltammograms (Figure 12b) show the features of weakly adsorbed hydrogen on TPPTP-caped Pt nanoparticles (dotted curve). They attribute this observation to the surface ligands that change the electronic energy of the Pt frontier orbitals and hence alter the hydrogen adsorption electrochemistry. More importantly, the TPPTP ligands weaken the oxygen adsorption on Pt, as evidenced by the positive shift of 40 mV for both onset potential and reduced desorption peak of oxygen species, as compared to that on a "bare" Pt/VC catalyst with a similar core size of 2.4 nm (solid curve). The weakening of the Pt–O bonds may improve the ORR electrocatalytic activity, since the reduced desorption of oxygen species is the rate-determined step for ORR on Pt.[7] Figure 12c and d show the polarization curves and Tafel plots of area-specific ORR activities for these Pt catalysts (along with a somewhat larger "bare" Pt/VC sample of about 4.4 nm in diameter) in O_2-saturated 0.1 M $HClO_4$ with a rotating disc electrode. The area-specific activity of TPPTP-caped Pt is enhanced by 22% in comparison with naked Pt; however, the mass-specific activity is inferior due to lower specific electrochemical area, as shown in Figure 12c. Two factors may contribute to the enhancement in area-specific activity. One is the weakening of Pt-O bonds, as mentioned above, and the other is hydrophobic effect of the aryl groups in TPPTP, which may repel water and inhibit Pt-oxide formation.

Thiol molecules have also be used to functionalize Pt nanoparticles,[56-58] but no considerable improvement of the ORR activity has been achieved.

4. Conclusion

In this chapter, we highlight some new progress in the study of the impacts of deliberate chemical functionalization of massive single crystal planes and noble metal nanoparticles with specific molecules, ions and molecular fragments on their catalytic performance in fuel cell electrochemistry. Through the interactions between the modifying groups and reactants (or spectator molecules/ions), and ligand-mediated electronic effects, the electrocatalytic activity and selectivity may be greatly tuned. This approach may have extensive applications in analytical, synthetic and materials chemistry as well as in chemical energy conversion and storage, and selective fuel production.

Further studies in this field may include the following aspects: (1) selection and optimization of functional molecules that can greatly change surface electronic structure of the metal substrates, but not occupy too many metal surface sites; (2) improvement of the stability of the modifying molecules, especially under the electrochemical conditions for ORR; (3) exploration of functional molecules that have synergistic effects for target reactions; and (4) identification of modifying molecules that possess special physicochemical properties, such as high solubility for O_2, great hydrophilic or hydrophobic characteristics, and an environment similar to enzyme, that are optimal for fuel cell electrocatalysis.

5. Acknowledgments

The authors are grateful to the National Science Foundation and the ACS-Petroleum Research Funds for financial supports of the research activities.

6. References

[1] Gasteiger, H. A.; Kocha, S. S.; Sompalli, B.; Wagner, F. T., Activity benchmarks and requirements for Pt, Pt-alloy, and non-Pt oxygen reduction catalysts for PEMFCs. *Applied Catalysis B-Environmental* 2005, 56, (1-2), 9-35.

[2] Liu, H. S.; Song, C. J.; Zhang, L.; Zhang, J. J.; Wang, H. J.; Wilkinson, D. P., A review of anode catalysis in the direct methanol fuel cell. *Journal of Power Sources* 2006, 155, (2), 95-110.

[3] Lim, B.; Jiang, M. J.; Camargo, P. H. C.; Cho, E. C.; Tao, J.; Lu, X. M.; Zhu, Y. M.; Xia, Y. A., Pd-Pt Bimetallic Nanodendrites with High Activity for Oxygen Reduction. *Science* 2009, 324, (5932), 1302-1305.

[4] Bing, Y. H.; Liu, H. S.; Zhang, L.; Ghosh, D.; Zhang, J. J., Nanostructured Pt-alloy electrocatalysts for PEM fuel cell oxygen reduction reaction. *Chemical Society Reviews* 2010, 39, (6), 2184-2202.

[5] Stamenkovic, V. R.; Fowler, B.; Mun, B. S.; Wang, G. F.; Ross, P. N.; Lucas, C. A.; Markovic, N. M., Improved oxygen reduction activity on Pt3Ni(111) via increased surface site availability. *Science* 2007, 315, (5811), 493-497.

[6] Zhang, J.; Sasaki, K.; Sutter, E.; Adzic, R. R., Stabilization of platinum oxygen-reduction electrocatalysts using gold clusters. *Science* 2007, 315, (5809), 220-222.

[7] Greeley, J.; Stephens, I. E. L.; Bondarenko, A. S.; Johansson, T. P.; Hansen, H. A.; Jaramillo, T. F.; Rossmeisl, J.; Chorkendorff, I.; Norskov, J. K., Alloys of platinum and early transition metals as oxygen reduction electrocatalysts. *Nature Chemistry* 2009, 1, (7), 552-556.

[8] Koh, S.; Strasser, P., Electrocatalysis on bimetallic surfaces: Modifying catalytic reactivity for oxygen reduction by voltammetric surface dealloying. *Journal of the American Chemical Society* 2007, 129, (42), 12624-+.

[9] Adzic, R. R.; Zhang, J.; Sasaki, K.; Vukmirovic, M. B.; Shao, M.; Wang, J. X.; Nilekar, A. U.; Mavrikakis, M.; Valerio, J. A.; Uribe, F., Platinum monolayer fuel cell electrocatalysts. *Topics in Catalysis* 2007, 46, (3-4), 249-262.

[10] Watanabe, M.; Motoo, S., Electrocatalysis by Ad-Atoms .2. Enhancement of Oxidation of Methanol on Platinum by Ruthenium Ad-Atoms. *Journal of Electroanalytical Chemistry* 1975, 60, (3), 267-273.

[11] Iwasita, T.; Hoster, H.; John-Anacker, A.; Lin, W. F.; Vielstich, W., Methanol oxidation on PtRu electrodes. Influence of surface structure and Pt-Ru atom distribution. *Langmuir* 2000, 16, (2), 522-529.

[12] Gasteiger, H. A.; Markovic, N.; Ross, P. N.; Cairns, E. J., Methanol Electrooxidation on Well-Characterized Pt-Rn Alloys. *Journal of Physical Chemistry* 1993, 97, (46), 12020-12029.

[13] Toda, T.; Igarashi, H.; Watanabe, M., Role of electronic property of Pt and Pt alloys on electrocatalytic reduction of oxygen. *Journal of the Electrochemical Society* 1998, 145, (12), 4185-4188.

[14] Paulus, U. A.; Wokaun, A.; Scherer, G. G.; Schmidt, T. J.; Stamenkovic, V.; Radmilovic, V.; Markovic, N. M.; Ross, P. N., Oxygen reduction on carbon-supported Pt-Ni and Pt-Co alloy catalysts. *Journal of Physical Chemistry B* 2002, 106, (16), 4181-4191.

[15] Tian, N.; Zhou, Z. Y.; Sun, S. G.; Ding, Y.; Wang, Z. L., Synthesis of tetrahexahedral platinum nanocrystals with high-index facets and high electro-oxidation activity. *Science* 2007, 316, (5825), 732-735.

[16] Vidal-Iglesias, F. J.; Solla-Gullon, J.; Rodriguez, P.; Herrero, E.; Montiel, V.; Feliu, J. M.; Aldaz, A., Shape-dependent electrocatalysis: ammonia oxidation on platinum nanoparticles with preferential (100) surfaces. *Electrochemistry Communications* 2004, 6, (10), 1080-1084.

[17] Zhang, J.; Yang, H. Z.; Fang, J. Y.; Zou, S. Z., Synthesis and Oxygen Reduction Activity of Shape-Controlled Pt(3)Ni Nanopolyhedra. *Nano Letters* 2010, 10, (2), 638-644.

[18] Xia, Y. N.; Xiong, Y. J.; Lim, B.; Skrabalak, S. E., Shape-Controlled Synthesis of Metal Nanocrystals: Simple Chemistry Meets Complex Physics? *Angewandte Chemie-International Edition* 2009, 48, (1), 60-103.

[19] Susut, C.; Chapman, G. B.; Samjeske, G.; Osawa, M.; Tong, Y., An unexpected enhancement in methanol electro-oxidation on an ensemble of Pt(111) nanofacets: a case of nanoscale single crystal ensemble electrocatalysis. *Physical Chemistry Chemical Physics* 2008, 10, (25), 3712-3721.

[20] Mazumder, V.; Sun, S. H., Oleylamine-Mediated Synthesis of Pd Nanoparticles for Catalytic Formic Acid Oxidation. *Journal of the American Chemical Society* 2009, 131, (13), 4588-+.

[21] Murray, R. W., Chemically Modified Electrodes. *Accounts of Chemical Research* 1980, 13, (5), 135-141.

[22] Abruna, H. D., Coordination Chemistry in 2 Dimensions - Chemically Modified Electrodes. *Coordination Chemistry Reviews* 1988, 86, 135-189.

[23] Dong, S. J.; Wang, Y. D., The Application of Chemically Modified Electrodes in Analytical-Chemistry. *Electroanalysis* 1989, 1, (2), 99-106.

[24] Clavilier, J.; Faure, R.; Guinet, G.; Durand, R., Preparation of Mono-Crystalline Pt Microelectrodes and Electrochemical Study of the Plane Surfaces Cut in the Direction of the (111) and (110) Planes. *Journal of Electroanalytical Chemistry* 1980, 107, (1), 205-209.

[25] Sun, S. G.; Clavilier, J.; Bewick, A., The Mechanism of Electrocatalytic Oxidation of Formic-Acid on Pt (100) and Pt (111) in Sulfuric-Acid Solution - An Emirs Study. *Journal of Electroanalytical Chemistry* 1988, 240, (1-2), 147-159.

[26] Borup, R.; Meyers, J.; Pivovar, B.; Kim, Y. S.; Mukundan, R.; Garland, N.; Myers, D.; Wilson, M.; Garzon, F.; Wood, D.; Zelenay, P.; More, K.; Stroh, K.; Zawodzinski, T.; Boncella, J.; McGrath, J. E.; Inaba, M.; Miyatake, K.; Hori, M.; Ota, K.; Ogumi, Z.; Miyata, S.; Nishikata, A.; Siroma, Z.; Uchimoto, Y.; Yasuda, K.; Kimijima, K. I.; Iwashita, N., Scientific aspects of polymer electrolyte fuel cell durability and degradation. *Chemical Reviews* 2007, 107, (10), 3904-3951.

[27] Genorio, B.; Strmcnik, D.; Subbaraman, R.; Tripkovic, D.; Karapetrov, G.; Stamenkovic, V. R.; Pejovnik, S.; Markovic, N. M., Selective catalysts for the hydrogen oxidation and oxygen reduction reactions by patterning of platinum with calix 4 arene molecules. *Nature Materials* 2010, 9, (12), 998-1003.

[28] Genorio, B.; Subbaraman, R.; Strmcnik, D.; Tripkovic, D.; Stamenkovic, V. R.; Markovic, N. M., Tailoring the Selectivity and Stability of Chemically Modified Platinum Nanocatalysts To Design Highly Durable Anodes for PEM Fuel Cells. *Angewandte Chemie-International Edition* 2011, 50, (24), 5468-5472.

[29] Stickney, J. L.; Rosasco, S. D.; Salaita, G. N.; Hubbard, A. T., Ordered Ionic Layers Formed on Pt(111) from Aqueous-Solutions. *Langmuir* 1985, 1, (1), 66-71.

[30] Stuhlmann, C.; Villegas, I.; Weaver, M. J., Scanning-Tunneling-Microscopy and Infrared-Spectroscopy as Combined in-Situ Probes of Electrochemical Adlayer Structure - Cyanide on Pt(111). *Chemical Physics Letters* 1994, 219, (3-4), 319-324.

[31] Huerta, F.; Morallon, E.; Quijada, C.; Vazquez, J. L.; Berlouis, L. E. A., Potential modulated reflectance spectroscopy of Pt(111) in acidic and alkaline media: cyanide adsorption. *Journal of Electroanalytical Chemistry* 1999, 463, (1), 109-115.

[32] Cuesta, A., At least three contiguous atoms are necessary for CO formation during methanol electrooxidation on platinum. *Journal of the American Chemical Society* 2006, 128, (41), 13332-13333.

[33] Strmcnik, D.; Escudero-Escribano, M.; Kodama, K.; Stamenkovic, V. R.; Cuesta, A.; Markovic, N. M., Enhanced electrocatalysis of the oxygen reduction reaction based on patterning of platinum surfaces with cyanide. *Nature Chemistry* 2010, 2, (10), 880-885.

[34] Macia, M. D.; Campina, J. M.; Herrero, E.; Feliu, J. M., On the kinetics of oxygen reduction on platinum stepped surfaces in acidic media. *Journal of Electroanalytical Chemistry* 2004, 564, (1-2), 141-150.

[35] Strmcnik, D.; Kodama, K.; van der Vliet, D.; Greeley, J.; Stamenkovic, V. R.; Markovic, N. M., The role of non-covalent interactions in electrocatalytic fuel-cell reactions on platinum. *Nature Chemistry* 2009, 1, (6), 466-472.

[36] Allongue, P.; Delamar, M.; Desbat, B.; Fagebaume, O.; Hitmi, R.; Pinson, J.; Saveant, J. M., Covalent modification of carbon surfaces by aryl radicals generated from the electrochemical reduction of diazonium salts. *Journal of the American Chemical Society* 1997, 119, (1), 201-207.

[37] Jiang, D. E.; Sumpter, B. G.; Dai, S., Structure and bonding between an aryl group and metal surfaces. *Journal of the American Chemical Society* 2006, 128, (18), 6030-6031.

[38] Mirkhalaf, F.; Paprotny, J.; Schiffrin, D. J., Synthesis of metal nanoparticles stabilized by metal-carbon bonds. *Journal of the American Chemical Society* 2006, 128, (23), 7400-7401.

[39] Ghosh, D.; Chen, S. W., Palladium nanoparticles passivated by metal-carbon covalent linkages. *Journal of Materials Chemistry* 2008, 18, (7), 755-762.

[40] Laurentius, L.; Stoyanov, S. R.; Gusarov, S.; Kovalenko, A.; Du, R. B.; Lopinski, G. P.; McDermott, M. T., Diazonium-Derived Aryl Films on Gold Nanoparticles: Evidence for a Carbon-Gold Covalent Bond. *Acs Nano* 2011, 5, (5), 4219-4227.

[41] Zhou, Z. Y.; Kang, X. W.; Song, Y.; Chen, S. W., Butylphenyl-functionalized palladium nanoparticles as effective catalysts for the electrooxidation of formic acid. *Chemical Communications* 2011, 47, (21), 6075-6077.

[42] Hostetler, M. J.; Wingate, J. E.; Zhong, C. J.; Harris, J. E.; Vachet, R. W.; Clark, M. R.; Londono, J. D.; Green, S. J.; Stokes, J. J.; Wignall, G. D.; Glish, G. L.; Porter, M. D.; Evans, N. D.; Murray, R. W., Alkanethiolate gold cluster molecules with core diameters from 1.5 to 5.2 nm: Core and monolayer properties as a function of core size. *Langmuir* 1998, 14, (1), 17-30.

[43]Lin-Vien, D.; Colthup, N. B.; Fateley, W. G.; Grasselli, J. G., *The Handbook of Infrared and Raman Characteristics Frequencies of Organic Molecules*. Academic Press: New York, 1991.

[44] Hoshi, N.; Kagaya, K.; Hori, Y., Voltammograms of the single-crystal electrodes of palladium in aqueous sulfuric acid electrolyte: Pd(S)- n(111) x (111) and Pd(S)-n(100) x (111). *Journal of Electroanalytical Chemistry* 2000, 485, (1), 55-60.

[45] Zhou, Z. Y.; Ren, J.; Kang, X. W.; Song, Y.; Sun, S. G.; Chen, S. W., Butylphenyl-Functionalized Pt Nanoparticles as CO-Resistent Electrocatalysts for Formic Acid Oxidation. *Physical Chemistry Chemical Physics 2012, 14 (4), 1412-1417*

[46] Adenier, A.; Combellas, C.; Kanoufi, F.; Pinson, J.; Podvorica, F. I., Formation of polyphenylene films on metal electrodes by electrochemical reduction of benzenediazonium salts. *Chemistry of Materials* 2006, 18, (8), 2021-2029.

[47] Kariuki, J. K.; McDermott, M. T., Nucleation and growth of functionalized aryl films on graphite electrodes. *Langmuir* 1999, 15, (19), 6534-6540.

[48] Capon, A.; Parsons, R., Oxidation of Formic-Acid at Noble-Metal Electrodes Part .3. Intermediates and Mechanism on Platinum-Electrodes. *Journal of Electroanalytical Chemistry* 1973, 45, (2), 205-231.

[49] Xia, X. H.; Iwasita, T., Influence of Underpotential Deposited Lead Upon the Oxidation of Hcooh in $HClO_4$ at Platinum-Electrodes. *Journal of the Electrochemical Society* 1993, 140, (9), 2559-2565.

[50] Leiva, E.; Iwasita, T.; Herrero, E.; Feliu, J. M., Effect of adatoms in the electrocatalysis of HCOOH oxidation. A theoretical model. *Langmuir* 1997, 13, (23), 6287-6293.

[51] Ye, E. Y.; Tan, H.; Li, S. P.; Fan, W. Y., Self-organization of spherical, core-shell palladium aggregates by laser-induced and thermal decomposition of Pd(PPh3)(4). *Angewandte Chemie-International Edition* 2006, 45, (7), 1120-1123.

[52] Son, S. U.; Jang, Y.; Yoon, K. Y.; Kang, E.; Hyeon, T., Facile synthesis of various phosphine-stabilized monodisperse palladium nanoparticles through the understanding of coordination chemistry of the nanoparticles. *Nano Letters* 2004, 4, (6), 1147-1151.

[53] Pietron, J. J.; Garsany, Y.; Baturina, O.; Swider-Lyons, K. E.; Stroud, R. M.; Ramaker, D. E.; Schull, T. L., Electrochemical observation of ligand effects on oxygen reduction at ligand-stabilized Pt nanoparticle electrocatalysts. *Electrochemical and Solid State Letters* 2008, 11, (8), B161-B165.

[54] Kostelansky, C. N.; Pietron, J. J.; Chen, M. S.; Dressick, W. J.; Swider-Lyons, K. E.; Ramaker, D. E.; Stroud, R. M.; Klug, C. A.; Zelakiewicz, B. S.; Schull, T. L., Triarylphosphine-stabilized platinum nanoparticles in three-dimensional nanostructured films as active electrocatalysts. *Journal of Physical Chemistry B* 2006, 110, (43), 21487-21496.

[55] Gatewood, D. S.; Schull, T. L.; Baturina, O.; Pietron, J. J.; Garsany, Y.; Swider-Lyons, K. E.; Ramaker, D. E., Characterization of ligand effects on water activation in triarylphosphine-stabilized Pt nanoparticle catalysts by X-ray absorption spectroscopy. *Journal of Physical Chemistry C* 2008, 112, (13), 4961-4970.

[56] Baret, B.; Aubert, P. H.; Mayne-L'Hermite, M.; Pinault, M.; Reynaud, C.; Etcheberry, A.; Perez, H., Nanocomposite electrodes based on pre-synthesized organically capped platinum nanoparticles and carbon nanotubes. Part I: Tuneable low platinum loadings, specific H upd feature and evidence for oxygen reduction. *Electrochimica Acta* 2009, 54, (23), 5421-5430.

[57] Cavaliere, S.; Raynal, F.; Etcheberry, A.; Herlem, M.; Perez, H., Direct electrocatalytic activity of capped platinum nanoparticles toward oxygen reduction. *Electrochemical and Solid State Letters* 2004, 7, (10), A358-A360.

[58] Cavaliere-Jaricot, S.; Haccoun, J.; Etcheberry, A.; Herlem, M.; Perez, H., Oxygen reduction of pre-synthesized organically capped platinum nanoparticles assembled in mixed Langmuir-Blodgett films: Evolutions with the platinum amount and leveling after fatty acid removal. *Electrochimica Acta* 2008, 53, (20), 5992-5999.

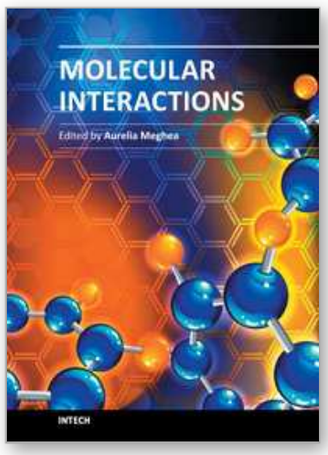

Molecular Interactions

Edited by Prof. Aurelia Meghea

ISBN 978-953-51-0079-9
Hard cover, 400 pages
Publisher InTech
Published online 29, February, 2012
Published in print edition February, 2012

In a classical approach materials science is mainly dealing with interatomic interactions within molecules, without paying much interest on weak intermolecular interactions. However, the variety of structures actually is the result of weak ordering because of noncovalent interactions. Indeed, for self-assembly to be possible in soft materials, it is evident that forces between molecules must be much weaker than covalent bonds between the atoms of a molecule. The weak intermolecular interactions responsible for molecular ordering in soft materials include hydrogen bonds, coordination bonds in ligands and complexes, ionic and dipolar interactions, van der Waals forces, and hydrophobic interactions. Recent evolutions in nanosciences and nanotechnologies provide strong arguments to support the opportunity and importance of the topics approached in this book, the fundamental and applicative aspects related to molecular interactions being of large interest in both research and innovative environments. We expect this book to have a strong impact at various education and research training levels, for young and experienced researchers from both academia and industry.

How to reference

In order to correctly reference this scholarly work, feel free to copy and paste the following:

Zhi-you Zhou and Shaowei Chen (2012). Impacts of Surface Functionalization on the Electrocatalytic Activity of Noble Metals and Nanoparticles, Molecular Interactions, Prof. Aurelia Meghea (Ed.), ISBN: 978-953-51-0079-9, InTech, Available from: http://www.intechopen.com/books/molecular-interactions/impacts-of-surface-functionalization-on-the-electrocatalytic-activity-of-noble-metals-and-nanopartic

INTECH
open science | open minds

InTech Europe
University Campus STeP Ri
Slavka Krautzeka 83/A
51000 Rijeka, Croatia
Phone: +385 (51) 770 447
Fax: +385 (51) 686 166
www.intechopen.com

InTech China
Unit 405, Office Block, Hotel Equatorial Shanghai
No.65, Yan An Road (West), Shanghai, 200040, China
中国上海市延安西路65号上海国际贵都大饭店办公楼405单元
Phone: +86-21-62489820
Fax: +86-21-62489821

IntechOpen